A Two Dimensional Analytical Evaluation of Thermal Fields during Metal Laser Sintering Processes

Chong Teng, Deepankar Pal, Haijun Gong, and Brent Stucker
Department of Industrial Engineering, University of Louisville, KY 40292

Abstract

Metal Laser Sintering (MLS) is a laser based manufacturing technique which is used for fabrication of parts in a layer-by-layer fashion using fine metal powders. Parts fabricated using MLS find wide applications in a myriad of areas such as medical, dental, and aerospace industries due to the availability of high geometric complexity, density, and their thermomechanical performance in service. A number of computational studies have been conducted in the past to help understand various underlying mechanisms related to laser melting and reconsolidation in order to arrive at strategies for better and faster machine architectures and process parameters combinations which result in stronger and longer-lasting parts.

As intellectual property barriers fall, due to expiring patents and more competitors licensed to produce machines, the desire to produce better next-generation machines is increasing. In addition there is a parallel realization that the industry needs better ways to develop new materials and control schemes for MLS processing. In order to achieve these goals, in this study we will provide an insight into the various thermo-mechanical phenomena which occur during MLS by providing a brief update on computational studies in the literature followed by the derivation of an efficient fully analytical framework for this problem. A two dimensional example is provided illustrating various aspects of this formulation which will be modified for a full 3 Dimensional formulation and implementation in the future to achieve the above-mentioned goals.

Introduction

Metal Laser Sintering (MLS), also known as Selective Laser Melting (SLM) has become more and more important because of the capacities of fabricating broad types of metals, processing parts with complex and subtle geometries, and resulting miscellaneous mechanical and thermal properties which could benefit all kinds of practical applications in industry. Even though SLM is a derivation of Selective Laser Sintering (SLS), it is generally more difficult to control because of issues with residual stress induced deformation, balling, incomplete powder melting, material phase changes, rapid solidification gradients and complex scan strategies for overlapping of melt pools [1, 2]. Therefore, understanding the underlying mechanisms in this Additive Manufacturing (AM) process is critical to optimization of process parameters, geometrical design and part qualification. Industry currently relies heavily on empirical testing and coupon fabrication in order to achieve better product quality. However, the high cost and long testing period for empirical testing illustrates the need for physics-based simulation and modeling of MLS processes.

In this paper, an analytical framework has been developed to investigate material transformation phenomena during MLS such as metal phase changes, melt pool size and temperature change with respect to different process parameters. In addition, latent heat energy provides information about physical processes which taking effect during laser beam heating in MLS [3]. Melt pool characteristics and the nonlinearity of thermal fields are critical issues in MLS processing and feedforward and feedback controls, particularly because of the large amount of laser energy released during a very short period of time [4]. In order to investigate these issues, a

two dimensional analytical approach is implemented using Matlab that will later be modified into a three dimensional formulation to assist in comparisons and validations of experimental results and to enable correlated simulation results using finite element analysis (FEA) in future work.

Mathematical Formulation

The general heat equation is given by thermal energy balance equation which is derived from the first law of thermodynamics. The change of enthalpy energy of a volume is equivalent to the total difference between internal energy change and external heat flux change:

$$\int_v \dot{H} \, dv = \int_v \dot{U} \, dv - \int_v \dot{F} \, dv \tag{1}$$

where H is enthalpy or heat content per unit volume, U is internal energy, and F is the heat flux. From Maxwell relations, the rate of enthalpy can be represented as:

$$\dot{H} = \rho C_v \frac{\partial T}{\partial t} \tag{2}$$

where ρ (kg/m^3) is the density, C_v (J/kg-K) is the specific heat capacity, and T (K) is the temperature. Also, from Fourier's law of heat conduction, the rate of heat flux is normally written as:

$$\dot{F} = \nabla(-k\nabla T) \tag{3}$$

where k (W/m-K) is the heat conductivity and ∇ is the gradient operator. The detailed derivations of above mentioned thermodynamics laws with thermodynamic potentials can be found in [5]. For a homogeneous medium, the spatial and time change of the internal energy remains in equilibrium such that:

$$\dot{U} = 0 \tag{4}$$

Substituting Eqs. (2), (3), and (4) into Equation (1), gives:

$$\rho C_v \frac{\partial T}{\partial t} = k\nabla^2 T \tag{5}$$

where the thermal diffusivity α (m^2/s) is defined as:

$$\alpha = \frac{k}{\rho C_v}$$

Equation (4) becomes:

$$\frac{\partial T}{\partial t} = \alpha(\nabla^2 T) \tag{6}$$

Equation (6) is widely used to govern the transient problem for a moving heat source [6-8]. If we only consider the moving source existing in the x-y plane, the two dimensional solution of Equation (6) becomes:

$$\Delta T(x, y, t) = \frac{Q_t}{(4\pi\alpha t)\rho C_v} e^{-\frac{x^2+y^2}{4\alpha t}} \qquad (7)$$

where Q_t (J/m) is the amount of heat liberated by the instantaneous point heat source through thickness at a period of t.

Laser Energy Modeling

A Gaussian model is the most common laser energy model used in MLS where a symmetric laser irradiance distribution is assumed across the laser beam [9]. By this definition, the heat flux is converted into expressions of laser parameters as [10]:

$$q(x, y) = \frac{2P}{\pi\omega^2} e^{-\frac{2(\omega_x^2+\omega_y^2)}{\omega^2}} \qquad (8)$$

where P (W) is the laser beam power, ω is the radius of the laser beam, and ω_x and ω_y are the distance between a point and the center of the laser beam in x and y directions. Integrating Equation (8) with respect to laser beam x and y dimensions, the total amount of heat Q (W) on the x-y plane becomes:

$$Q = \int_{x_{min}}^{x_{max}} \int_{y_{min}}^{y_{max}} q(x, y) dx dy$$

The laser absorptivity is typically assumed to be constant for a specific combination of laser wavelength, surface roughness, material and bed surface experimental temperature [11]. A typical EOS MLS machine, including the one used in this experiment, has a Yb-fibre laser wavelength of 1064 nm with a scan speed that is user-definable below 7.0 m/s. Due to the effects of laser absorptivity:

$$Q_{eff} = \beta Q$$

The effective laser absorptivity β for a 353 K powder bed temperature is assumed to be 0.76 for the powder layer and 0.35-0.4 for the underneath solid layer for Ti-6Al-4V [12]. Considering a 50 W Yb-fibre laser source with diameter of 100 μm scanning over a powder layer, the resulting Gaussian distribution of heat Q_{eff} is shown in Figure 1 with a peak power in the center of the laser center as 0.0940 W.
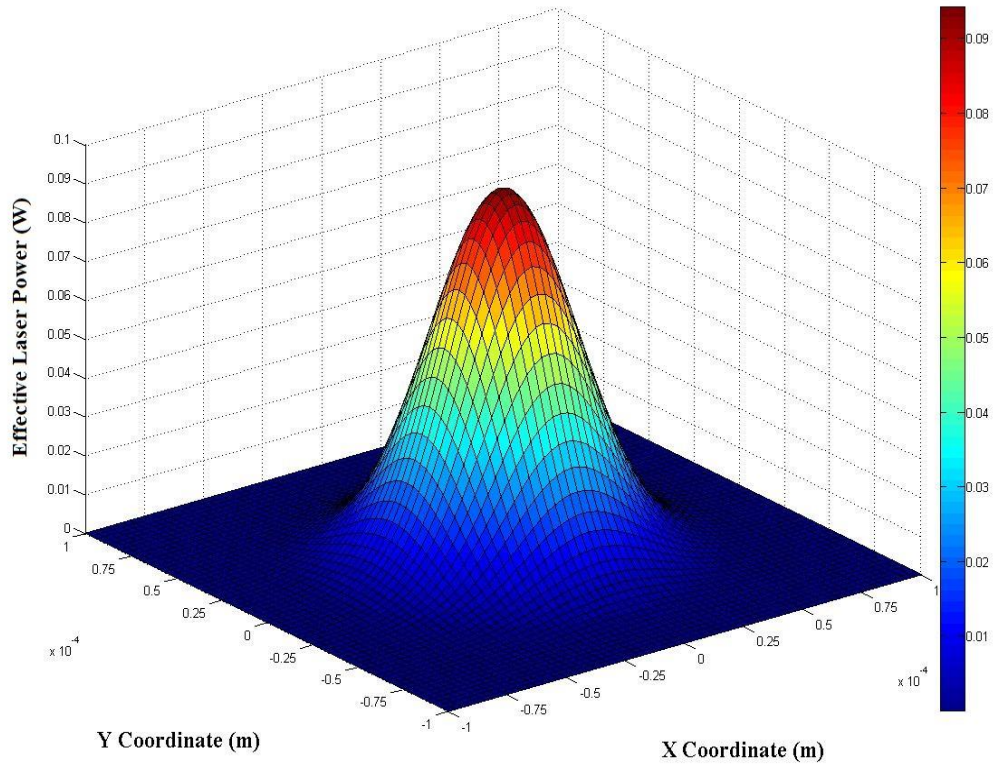
Figure 1: The Gaussian distribution of effective heat for a laser source with 50 W

Duhamel Integration

Solutions to the heat conduction problem (Equation (7)) by conventional methods is not possible when the heat flux is temperature dependent. However, Duhamel's theorem demonstrates that instead of solving Equation (7) directly, the solution can be expressed in terms of its fundamental solution using an simpler auxiliary problem [7]. In this case, we introduce a dummy parameter τ into Equation (7) based on the assumption that heat flux is not temperature dependent. The temperature rise caused by a moving laser source from 0 to t can be obtained by solving the following integration:

$$T = \int_0^t \frac{Q^*}{4\pi\alpha(t-\tau)\rho C_v} e^{-\frac{[x-v_x(t-\tau)]^2 + [y-v_y(t-\tau)]^2}{4\alpha(t-\tau)}} d\tau \qquad (9)$$

where v_x and v_y are the components of laser movement in x and y directions. For a two dimensional solution for Q^* (W/m), if we move the coordinate system with the laser source, point A at time t in the new coordinate system (X, Y) can be represented using its old coordinate (x, y) as $\left(X_A = x_A - v_x t, Y_A = y_A - v_y t\right)$, as shown in Figure 2.
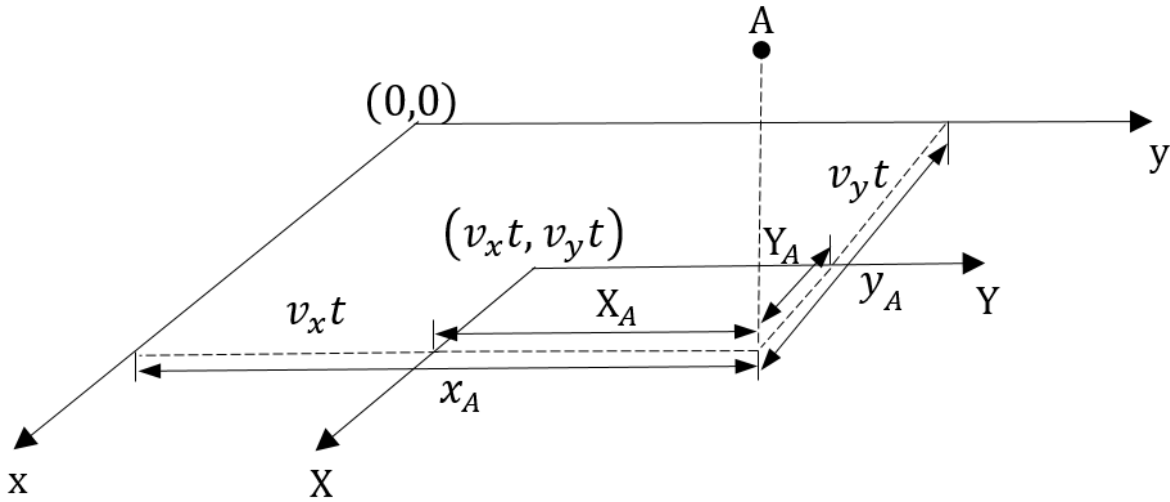
Figure 2: Coordinate transformation with respect to laser movement

The discontinuities of Duhamel's integration which normally result from different substep selections in applied boundary conditions, are dealt with in the literature by breaking the integration into several pieces [7]. In this paper, we used a superposition approach by treating the whole integration as a summation of piecewise solutions for each step τ_i [13]. For each step, the solution is equivalent to its mid position solution times distance. The representative solution of the integration in Equation (9) can be written as:

$$T = T_0 + \sum_{i=1}^{m} \frac{Q(\tau_i - \tau_{i-1})}{4\pi\alpha\left(t - \frac{\tau_i - \tau_{i-1}}{2}\right)\rho C_v} e^{-\frac{\left[x - v_x\left(t - \frac{\tau_i - \tau_{i-1}}{2}\right)\right]^2 + \left[y - v_y\left(t - \frac{\tau_i - \tau_{i-1}}{2}\right)\right]^2}{4\alpha\left(t - \frac{\tau_i - \tau_{i-1}}{2}\right)}} \tag{10}$$

In order to test if the temperature mismatch converges using Equation (10), we consider a Ti-6Al-4V solid with a 100 W laser source moving at 1.2 m/s and elements close to the laser region sized to be 10 μm × 10 μm, the corresponding material properties are plotted in Figure 4, Figure 5, and Figure 6. By choosing different $\Delta\tau$, after stabilization, the temperature fields are compared below in Figure 3. As we can observe, the temperature fields predicted by using different $\Delta\tau$ are very close to each other (maximum difference around 1%) which is good enough to prove that the convergence effects between each step are handled well by applying Equation (10).
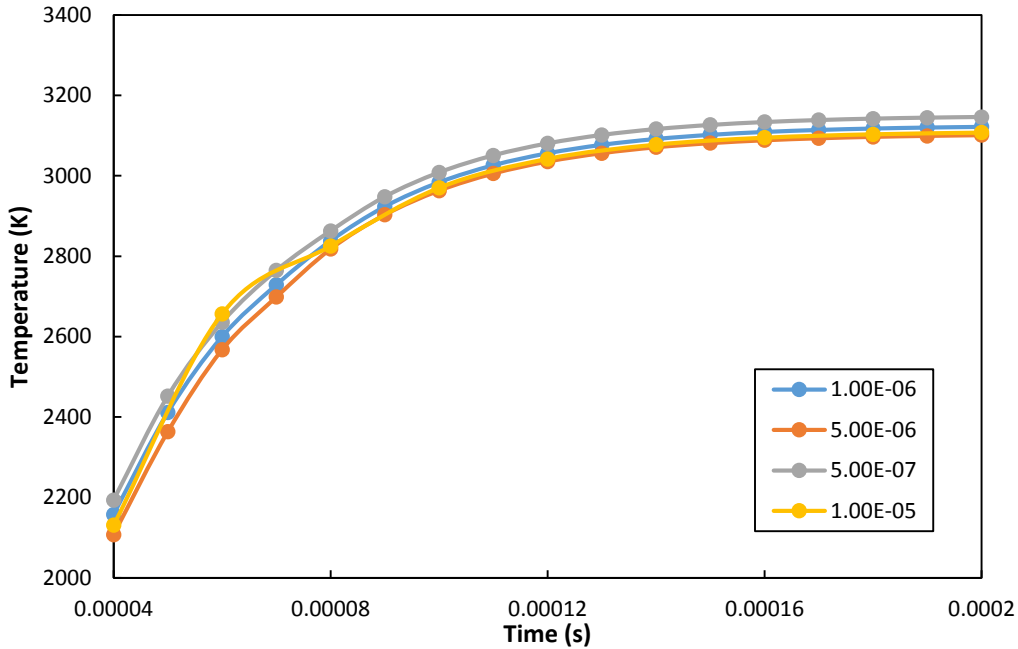
Figure 3: Temperature fields with respect to different $\Delta\tau$

Nonlinear Material Properties of Ti-6Al-4V

The material Ti-6Al-4V is used in this paper and the nonlinear temperature dependent material properties which have been obtained from [14] are shown in Figure 4, Figure 5, and Figure 6. The density decrease between 1800K and 2500K is caused by the material state change, and after that it becomes flat. The specific heat capacity and heat conductivity values drop down between 900K-1100K because of the material $\alpha \rightarrow \alpha' \rightarrow \beta$ phase transformations and keep increasing thereafter until the melting point, where it remains constant. The ratios between bulk and powder material properties for density, specific heat capacity, and heat conductivity are obtained from [15] where 1923K is used as the melting temperature of Ti-6Al-4V.
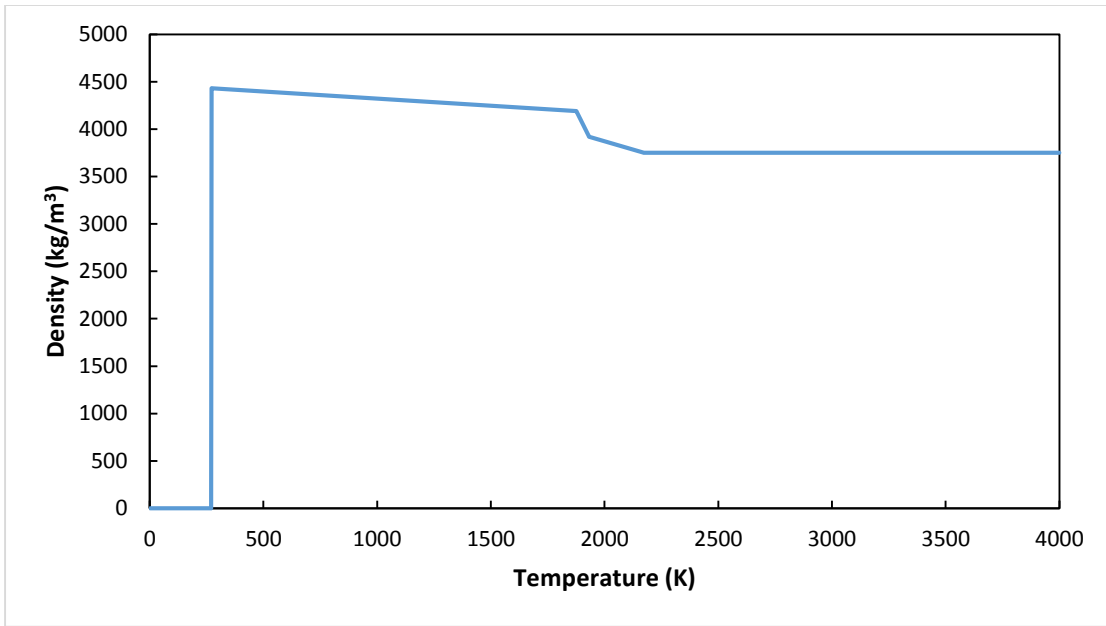
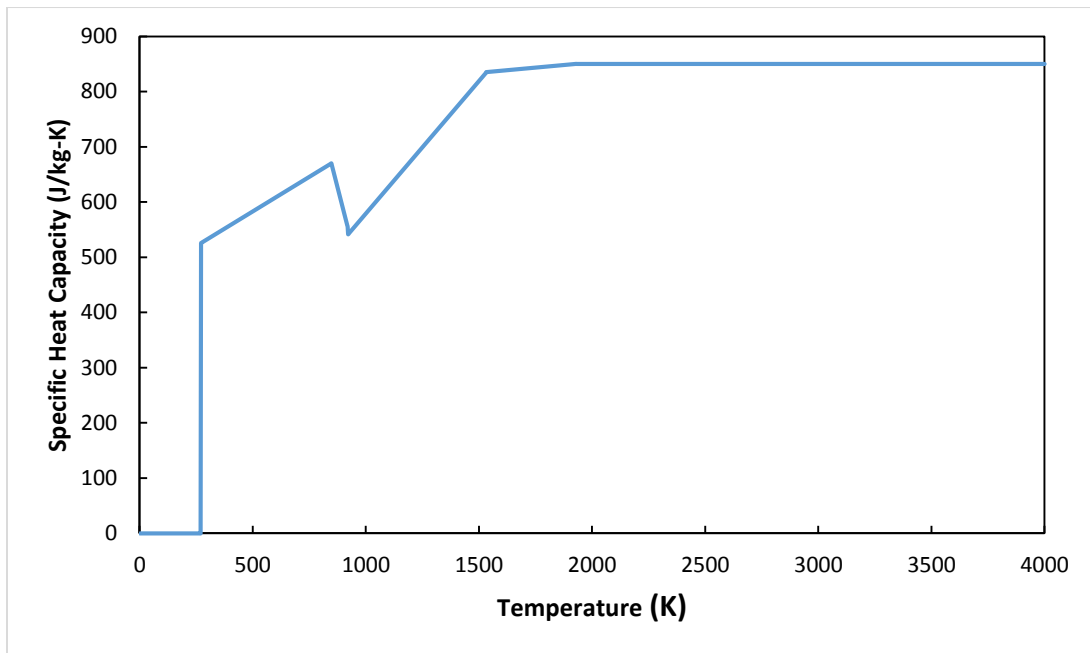Figure 4：Density of Ti-6Al-4V with respect to temperature

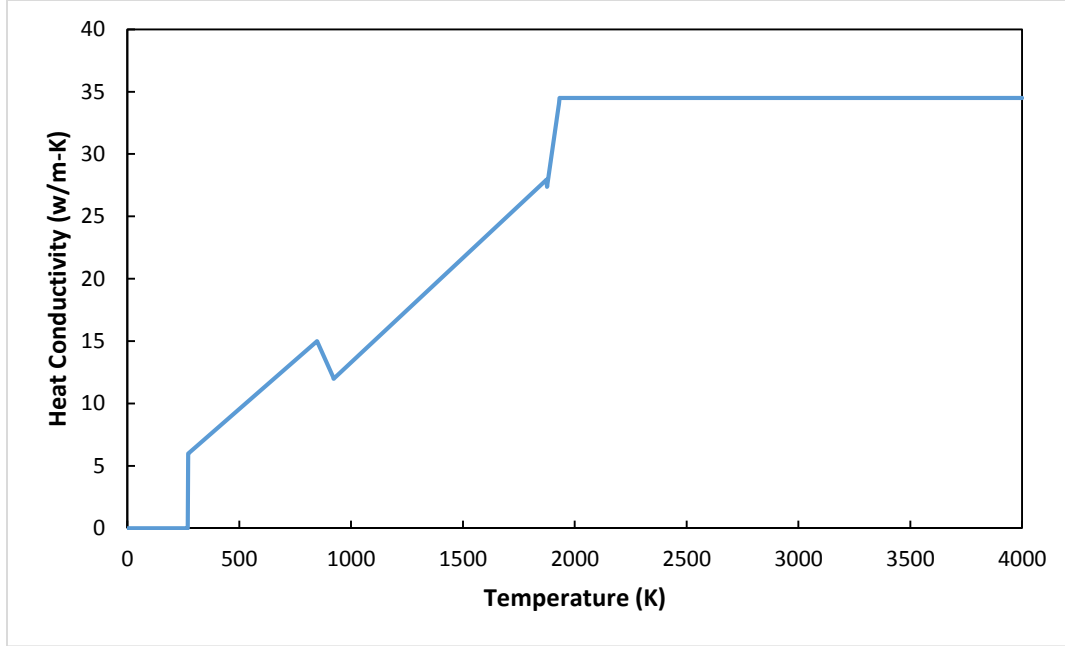Figure 5: Specific heat capacity of Ti-6Al-4V with respect to temperature

Figure 6: Thermal conductivity of Ti-6Al-4V with respect to temperature

Latent Heat

Latent heat is defined as the heat absorbed or released as a result of a material phase transformation. In the literature, several methodologies are available for taking into account latent heat effects induced by material phase changes, including the apparent heat capacity method [16], effective capacity method [17], heat integration method [18], source based method [19], and enthalpy method [20]. A review of these methods is given in [21]. In this paper, the following equation was used to take care of the heat capacity change during material phase change:

$$C(T) = C_s + \frac{L_f\{T-T_s\}}{\Delta T_f^2} + \frac{L_v\{T-T_m\}}{\Delta T_v^2} \tag{11}$$

where C_s is the specific heat capacity of the material at the solidus temperature, L_f (J/kg) is the latent heat of fusion, L_v is the latent heat of vaporization, T_s is the solidus temperature, T_m is the melting temperature, $\Delta T_f = T_m - T_s$, T_v is the vaporization temperature, $\Delta T_v = T_v - T_m$, and $\{\}$ is the Macaulay brackets (enclosed expression maintains the value when the expression stays non-negative while it goes to zero when negative). In order to keep the balance of force, in our problem the heat Q_L caused by latent heat can be obtained by:

$$Q_L(t) = \rho_t L_t v_t \tag{12}$$

where during phase change quantities: ρ_t (kg/m^2) is the area density of the material at time t, L_t is the amount of latent heat at time t, and v_t (m/s) is the solidified interface velocity. Substituting Equation (11) and (12) into Equation (10), we can calculate the temperature decrease caused by a material phase change. As we can see, the latent heat is related with the laser energy input induced temperature rise and the corresponding solidified interface movement. A sensitivity analysis is carried out by assuming a Ti-6Al-4V solid experiences a phase change from its solidus temperature

1152

1873 K to its liquidus temperature 1923K, the resulting temperature decrease by latent heat with different solidified interface velocity is shown in Figure 7.
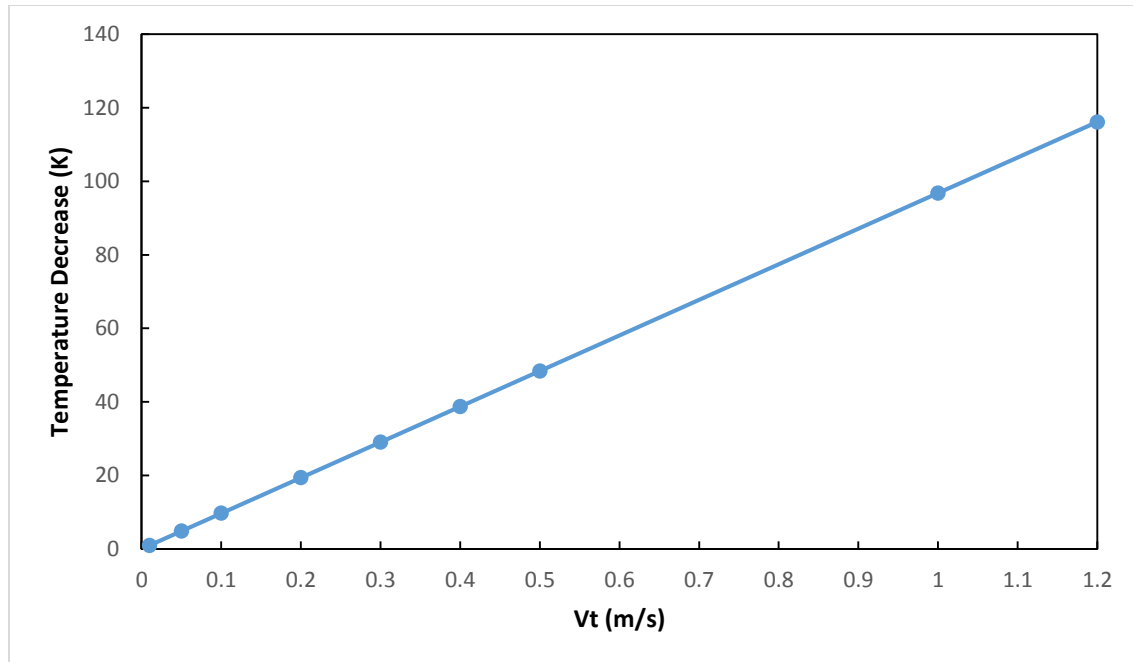

Figure 7: The latent heat induced temperature decrease with respect to different solidified interface velocities of Ti-6Al-4V

Thermal Fields Results

In MLS, the temperature field around the laser beam is highly nonlinear and the thermal wave is hard to predict accurately because the temperature is obtained based on a step by step calculation with temperature dependent material properties. This issue is exacerbated by the laser beam characteristics of a large amount of energy applied to a very small area for a short period of time. Thus the temperature rise and subsequent material property changes used in the calculation are large. The relationships of peak temperature for a Ti-6Al-4V solid part with different process parameters such as laser power and scan speed are shown in Figure 8 and Figure 9. In Figure 8, the scan speed of the laser beam is kept constant at 1.2 m/s while in Figure 9, the laser power of the beam is kept constant at 75 W.

A case study was carried out in order to investigate the accuracy of this thermal solution. A 125 W laser beam moving at a speed of 1.2 m/s along the positive x direction and temperature dependent material properties of Ti-6Al-4V were used. The shape of the melt pool was assumed to be half of the ellipsoid volume in order to convert the laser beam energy into the corresponding planar energy. The laser is assumed to scan directly on the base plate in order to minimize possible error created from through thickness cooling (this effect is dominant in powder on top of solid melting and solidification processes) since this is a two dimensional rather than three dimensional solution. The in-plane thermal contour and three dimensional thermal surface plot for laser beam movement of 200 μm are shown in Figure 10 and Figure 11. It was found that the melt pool size is about 100 μm and the peak temperature is about 4500K at this time step while the peak temperature increases slowly until it hits the value shown in Figure 8.
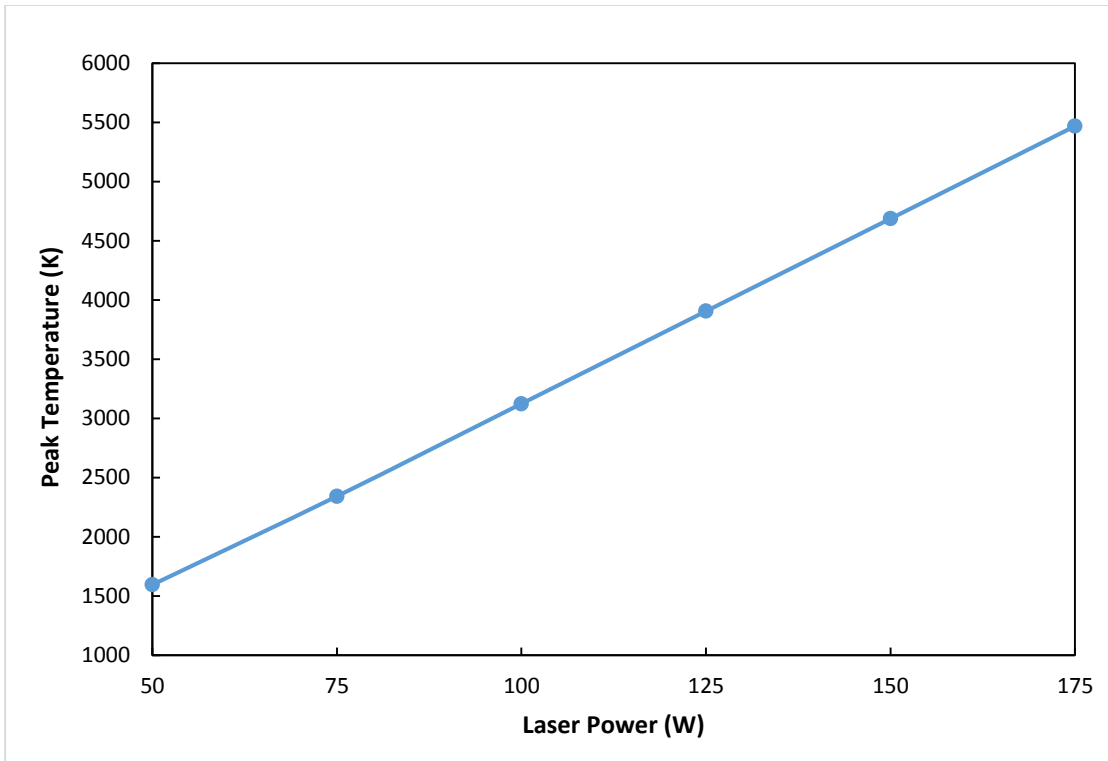
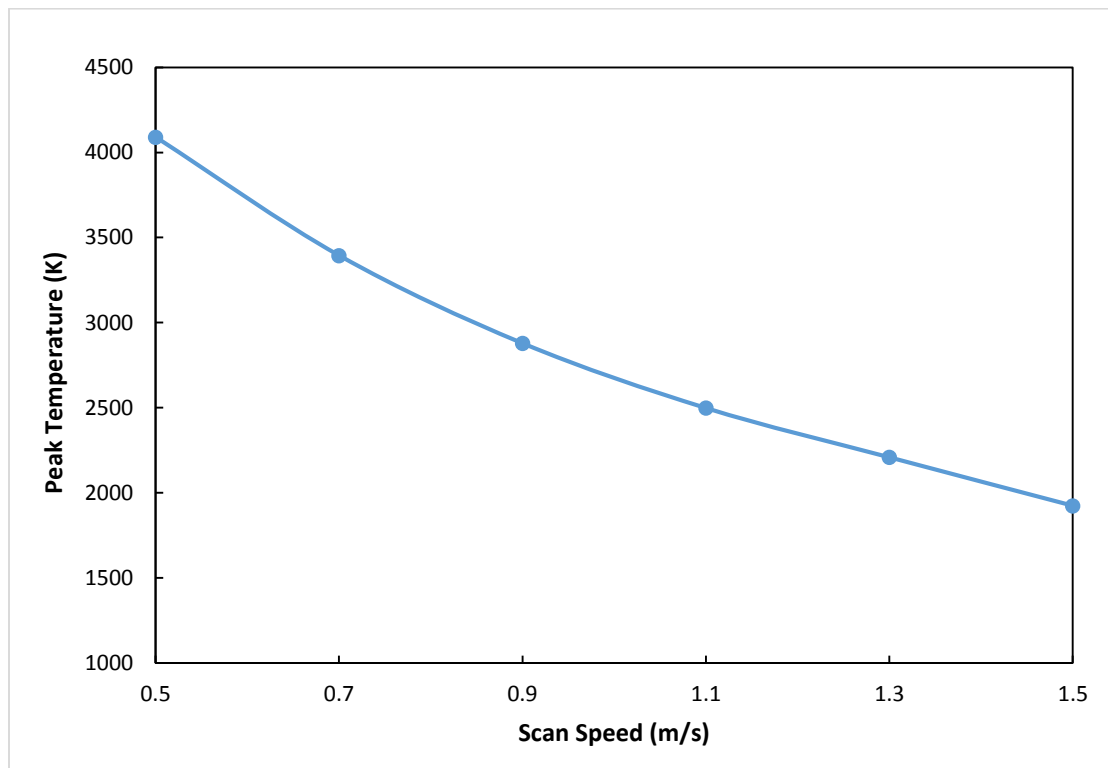Figure 8: Laser power effects on peak temperature
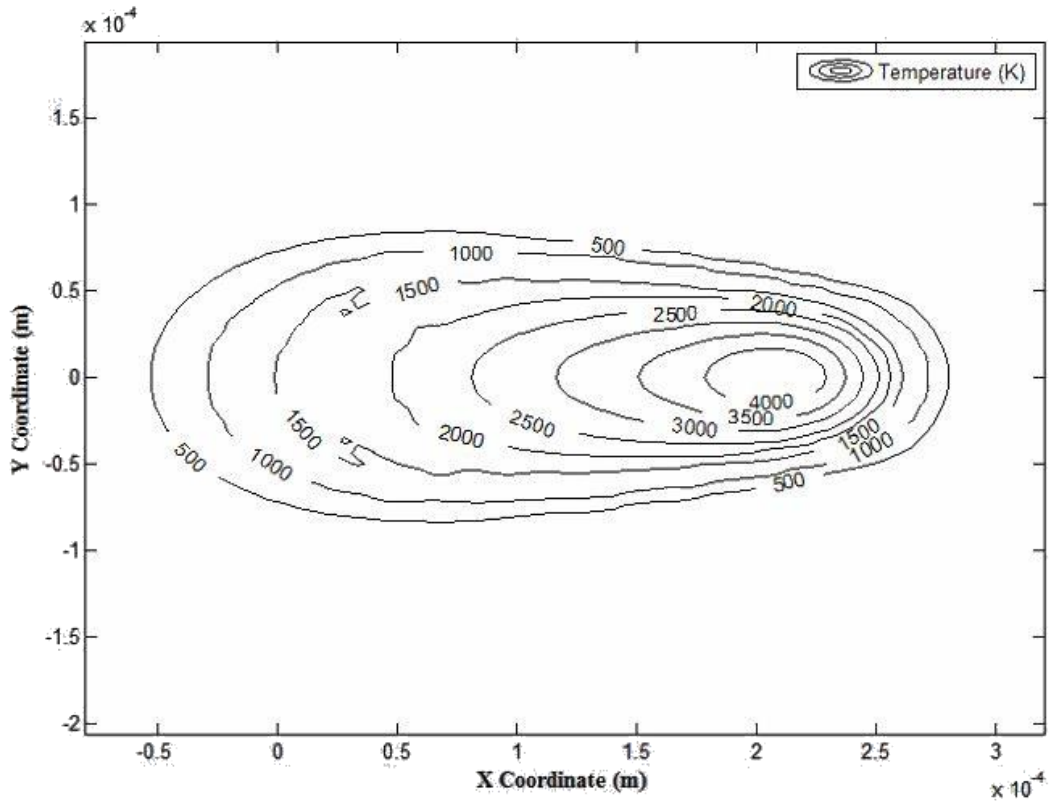

Figure 9: Scan speed effects on peak temperature

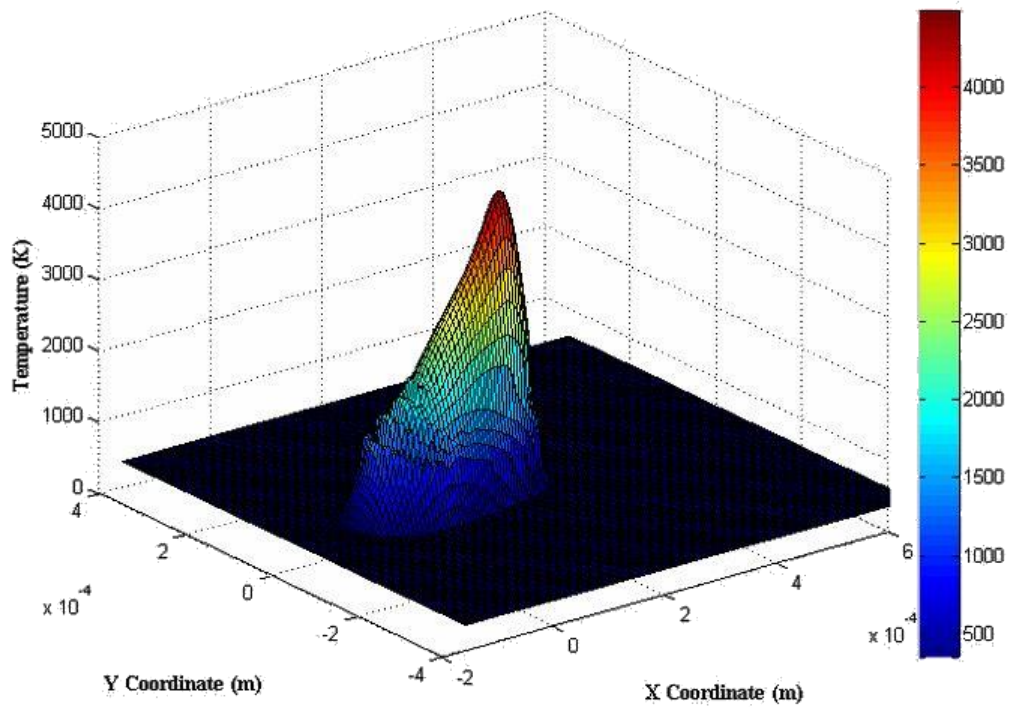Figure 10: Thermal contour of a 125 W 1.2 m/s laser moving 200 μm in distance

Figure 11: 3D Thermal surface plot of a 125 W 1.2 m/s laser moving 200 μm distance

Conclusion and Future Work

A two dimensional analytical solution of thermal fields in metal laser sintering has been developed and implemented into Matlab to enable future validation of FEA solutions and verification against experiment results. The Duhamel integration method along with a solution for the convergence mismatch effect of the superposition approach was applied, and the maximum temperature deviation when using different substeps was greatly reduced to about 1% maximum. The material phase change induced latent heat energy was taken into account using a correlation between solidified interface velocity and temperature decrease. The peak temperature variation for different process parameters such as laser power and scan speed are shown. A case study shows the ability to predict thermal contours and melt pool shapes, but since the input energy is transformed into a planar energy, it is hard to compare this method with experimental results until a three dimensional model is completed. Most of the results provided in this paper are based on to the assumption of a laser moving across a solid base plate, which melts and solidifies in order to avoid possible errors resulting from superimposing some type of through thickness cooling assumption between powder and solid since this model is valid only for a two dimensional solution. Nevertheless, the predicted shapes of the melt pool and the thermal contours after melt pool stabilization from this case study look very much like observed phenomena from experiments.

In order to accurately compare the thermal field with experiment results, the machine operating temperature field needs to be investigated. The results and computational time using this approach are highly dependent on the mesh density and mesh quality; thus adaptive mesh refinement strategies (AMR) are favored at this point. Multiscale dynamic meshing has been previously developed [14], so with appropriate implementation of such mesh refinement methods, the current approach can be greatly improved.

A three dimensional analytical approach is being derived based on the approach demonstrated in this paper in order to achieve a more complete and accurate solution and the ability to do experimental validation. In addition, this three dimensional analytical solution will also ease the possible implementation of wavelet propagation approaches for MLS process modeling and simulation for pursuing even faster, more accurate MLS process modeling.

Reference

1. Kruth, J.-P., et al., *Selective Laser Melting of Iron-based Powder.* Journal of Materials Processing Technology, 2004. **149**(1): p. 616-622.
2. Kruth, J.-P., et al., *Binding Mechanisms in Selective Laser Sintering and Selective Laser Melting.* Rapid Prototyping Journal, 2005. **11**(1): p. 26-36.
3. Shuja, S.Z., B.S. Yilbas, and O. Momin, *Laser Heating of Moving Solid: Influence of Workpiece Speed on Melt Size.* AIChE Journal, 2010. **56**(11): p. 2997-3004.
4. Fox, J. and J. Beuth. *Process Mapping of Transient Melt Pool Response in Wire Feed E-Beam Additive Manufacturing of Ti-6Al-4V*. in *Solid Freeform Fabrication Symposium, Austin, TX*. 2013.
5. Teng, C., *Variational Asymptotic Method for Unit Cell Homogenization of Thermomechanical Behavior of Composite Materials*. 2014, Utah State University.
6. Carslaw, H.S., J.C. Jaeger, and H. Feshbach, *Conduction of Heat in Solids.* Physics Today, 1962. **15**: p. 74.
7. Ozisik, M.N., *Heat Conduction*. 1993: John Wiley & Sons.
8. Gibson, I., D.W. Rosen, and B. Stucker, *Additive Manufacturing Technologies*. 2010: Springer.

9.   Roberts, I., et al., *A Three-Dimensional Finite Element Analysis of the Temperature Field during Laser Melting of Metal Powders in Additive Layer Manufacturing.* International Journal of Machine Tools and Manufacture, 2009. **49**(12): p. 916-923.

10.   Dai, K. and L. Shaw, *Finite Element Analysis of the Effect of Volume Shrinkage during Laser Densification.* Acta Materialia, 2005. **53**(18): p. 4743-4754.

11.   Kruth, J.-P., et al., *Lasers and Materials in Selective Laser Sintering.* Assembly Automation, 2003. **23**(4): p. 357-371.

12.   Eane, R.B., *Metal Powder Effects on Selective Laser Sintering*. 2002, The University of Leeds.

13.   Taler, J. and P. Duda, *Solving Direct and Inverse Heat Conduction Problems*. 2010: Springer.

14.   Pal, D., et al., *A Generalized Feed Forward Dynamic Adaptive Mesh Refinement and De-Refinement Finite Element Framework for Metal Laser Sintering: Part II (Non-Linear Thermal Simulations and Validations).* Journal of Manufacturing Science and Engineering, 2014. **under review**.

15.   Beeler, D., et al., *Air Force Research Laboratory Report No. AFRL-rX-WP-TR-2012-0510*. 2012: Copies may be ordered from the Air Force Research laboratory, Dayton, OH 45433.

16.   Hashemi, H. and C. Sliepcevich. *A Numerical Method for solving Two-Dimensional Problems of Heat Conduction with Change of Phase*. in *Chem. Eng. Prog. Symp. Series*. 1967.

17.   Poirier, D. and M. Salcudean, *On Numerical Methods used in Mathematical Modeling of Phase Change in Liquid Metals.* Journal of Heat Transfer, 1988. **110**(3): p. 562-570.

18.   Dusinberre, G., *Numerical Methods for Transient Heat Flow.* Trans. ASME, 1945. **67**(8): p. 703-712.

19.   Voller, V. and C. Swaminathan, *ERAL Source-based Method for Solidification Phase Change.* Numerical Heat Transfer, Part B Fundamentals, 1991. **19**(2): p. 175-189.

20.   Eyres, N., et al., *The Calculation of Variable Heat Flow in Solids.* Philosophical Transactions of the Royal Society of London. Series A, Mathematical and Physical Sciences, 1946. **240**(813): p. 1-57.

21.   Hu, H. and S.A. Argyropoulos, *Mathematical Modelling of Solidification and Melting: A Review.* Modelling and Simulation in Materials Science and Engineering, 1996. **4**(4): p. 371.